Elastic Modulus and Migration capability of Leukemia Cells k562 Suffered Drug Treatment

Kui Wang[1, 2#], Yuntian Xue[1, #], Ying Peng[1], Xiangchao Pang[4], Yuanjun Zhang[1], L.I. Ruiz-Ortega[1], Ye Tian[1], A. H. W. Ngan[2], Bin Tang[1, 3*]

[1]Department of Biomedical Engineering, Southern University of Science and Technology, Shenzhen, 518055, P. R. China

[2]Department of Mechanical Engineering, University of Hong Kong, Hong Kong, P. R. China

[3]Guangdong Provincial Key Laboratory of Cell Microenvironment and Disease Research, Shenzhen Key Laboratory of Cell Microenvironment

[4]College of Materials Science and Engineering, Central South University of Forestry and Technology, Changsha, 410004, P. R. China

*Corresponding author: Bin Tang, Doctor, Department of Biomedical Engineering, Southern University of Science and Technology, Shenzhen, 518055, P. R. China

[#]These authors contributed equally to the work

Tel: +86-0755-88018998; E-mail address: tangb@sustc.edu.cn

KEY POINTS

1. A system include optical tweezers and rate-jump model was employed to measure the elastic modulus of leukemia cell quantitatively.

2. The elastic modulus of K562 cells had a three-fold increase after treated by phorbol 12-myristate 13-acetate (PMA).

3. The K562 cells' migration capability decrease with increasing elastic modulus

ABSTRACT

Leukemia is a commonly seen disease caused by the abnormal differentiation of hematopoietic stem cells and blasting in bone marrow. Even though some drugs have been applied to treat the diseas clinically, the influence of these drugs on leukemia cells' biomechanical properties, which are closely related to complications like leukostasis or infiltration, is still unclear. Due to the non-adherent and viscoelastic nature of leukemia cells, accurate measurement of their elastic modulus is still a challenging issue. In this study, we adopted the rate-jump method together with optical tweezers indentation to accurately measure the elastic modulus of leukemia cells K562 after phorbol 12-myristate 13-acetate (PMA), all-trans retinoic acid (ATRA), Cytoxan (CTX), and Dexamethasone (DEX) treatment, respectively. We found that compared to the control sample, K562 cells treated by PMA showed nearly a threefold increase in elastic modulus, while samples treated with other drugs revealed no apparent changes. The transwell experiment results suggested that the K562 cells treated with PMA have the lowest migration capability. Besides, it was shown that the cytoskeleton protein gene α-tubulin and vimentin have a significant increase in expression after PMA treatment by qPCR. The results indicate that PMA has a significant influence on protein expression, stiffness, and migration ability of the leukemia cell K562, and may also play an important role in the leukostasis in Leukemia.

KEYWORDS: leukemia cells, stiffness, PMA, cytoskeleton, optical tweezers

INTRODUCTION

Leukemia is a group of cancers in which white blood cells proliferate up to plentiful immature differentiated cells and aggregate in the bone marrow and blood vessel. Leukemia cells are not directly life-threatening, while a vast amount of leukemia cells due to abnormal proliferation will induce various complications that may lead to the death of patients, for instance, the leukostasis and infiltration[1]. Leukostasis is a series of symptoms caused by slow blood stasis, vascular occlusion, and organ ischemia due to the stacking of leukemia cells in the blood vessel. Previous studies suggest that the leukostasis is tightly related to the deformability and migration ability of leukemia cells[2]. The infiltration is the results of the invasion of leukemia cells from the blood vessel to organs, which may lead to irreversible damage of organ. For both leukostasis and infiltration, the capability for cell migration and invasion plays a critical role.

The cells' mechanical properties closely relate to their migration and invasion, in which the cells need to change their shape significantly[3]. In this sense, cell mechanics is essential in understanding the pathology and clinical symptoms. The invasive breast cancers have lower elastic modulus than the noninvasive breast cancer cells and normal breast cells[4]. Ovarian

cancer cells have higher metastatic potential because their higher deformability leads to a significant increase in their ability to proliferate and migrate[5]. Even in several types of cancer, the deformability is a biomarker for assessing the risk of metastasis[6,7].

Nowadays, several kinds of drugs treated leukemia clinically are widely used, e.g., phorbol 12-myristate 13-acetate (PMA), all-trans retinoic acid (ATRA), Cytoxan (CTX), and Dexamethasone (DEX). PMA and ATRA induce the differentiation of leukemia cell by modifying the formation and distribution of the cytoskeleton[8], whereas CTX and DEX can lead to apoptosis of the leukemia cells through chemical toxicity[9]. After PMA treatment, leukemia cells differentiate to megakaryocytic accompany by changes in cell morphology, adhesive properties, cell growth arrest, and polyploidization[10]. Side effects of these drugs include leukostasis and relapse, which are tightly related to the physical properties of cells[11]. These drugs will modify the cytoskeleton of the leukemia cells in the treatment process and then affect the mechanical properties and behavior of cells. However, the mechanism for these changes is still ambiguous.

The biophysical properties of leukemia cells have been effectively exploited previously through different platforms and methods. Several methods, such as atomic force microscopy (AFM)[12], micropipette aspiration technique (MAT)[13], magnetic twisting cytometry (MTC)[14], particle tracking rheology (PTR)[15] and optical tweezers (OT)[16], have been

previously employed to measure the mechanical properties of leukemia cells. By atomic force microscopy (AFM), Islam et al. have found that Young's modulus of K562 and Jurkat cells will be increased from 0.42 ± 0.38 and 0.29 ± 0.21 kPa to 1.51 ± 1.29 and 1.10 ± 1.08 kPa after treated with daunorubicin (2 μM)[17]. Lam et al. also have found that the stiffness of both the myeloid and lymphoid leukemia cells would increase after chemotherapy by AFM measured[18]. The chronic lymphocytic leukemia cells from the patients needed a relatively long time to transit in the microfluidic device and exhibited higher stiffness than the lymphocytic cell from the nature people[19]. Zhou et al. have found that the stiffness of K562 and HL60 is significantly higher than the normal macrophage, monocyte, and granulocyte through the platform of optical tweezers[20]. However, the reported value for the stiffness of the leukemia cells usually had a large scatter, and such scatter might primarily due to the viscous effects of the cell structures and variations in the cell geometry, both of which are factors that can significantly affect the elastic modulus measurement.

The rate-jump model, based on the response during a sudden jump in the loading or straining rate, provides a reliable method to eliminate the viscoelastic effects on the elastic modulus calculation for viscoelastic materials in various test platforms[20,21]. In our previous work, we have combined the optical tweezers and the rate-jump model to measure the elastic modulus of cells[20]. In this study, we have explored the elastic

modulus of human leukemia cell line K562 treated with PMA, ATRA, CTX, and DEX, respectively. Based on the force-displacement curves obtained by the OT experiments, the elastic modulus of the cells was calculated using the rate-jump model to measure the quantitative elastic modulus of leukemia cells. We have further explored the relationship between drug and biophysics, drug and cell structure, drug, and cell migration. We expected that the present work can lead to a better understanding of the structure-properties relationship of leukemia cells and might be able to reveal the possible connections between the risk of the leukostasis and the cell mechanics after drug treatment.

MATERIALS AND METHODS

Cell culture and treatment with chemotherapeutic agents

Chronic myeloid leukemia cell line K562 (ATCC®CRL-3343, U. S. A.)was used and cultured in Roswell Park Memorial Institute (RPMI, Hyclone, U. S. A.) 1640 supplemented with 10% fetal bovine serum (FBS, Hyclone, U. S. A.), 100 U/mL penicillin and 100 μg/mL streptomycin (Beyotime, China) at 37°C in 5% CO_2. To minimize the influence of cell phase before the mechanical tests, cells were incubated in RPMI without FBS for 24h at 37°C to synchronize cells in the G0 phase. To rejuvenate the cells, after synchronizing to the G0 phase, FBS was added to the medium again, and cultured for 6h under the same conditions to prepare

for the drug treatment. K562 cells were treated with different clinical drugs, including two differentiation therapy drugs: phorbol 12-myristate 13-acetate (PMA) (10 μg/L) and all-trans retinoic acid (ATRA) (1 μM), and two chemotherapy drugs, Cytoxan (CTX) (0.1 μM) and Dexamethasone (DEX) (1 μM). All the drugs were purchased from Sigma-Aldrich and were applied to the prepared cell groups 24h before optical tweezers testing. The control group was firstly synchronized to the G0 phase and then cultured in complete culture medium for 30h.

Indentation measurement

All the indentation measurements were performed on an optical tweezers system (JPK NanoTrackerII, Bruker, U. S. A.). In this study, the laser power was controlled to be between 1W and 2W in order to avoid possible damage to cells. Polystyrene microbeads supplied by Polyscience Company with a diameter of 3.0 μm were used as "indenters". Firstly, the bottom of the petri dish was coated with a layer of Cell-Tak reagents (Corning, U. S. A.) (11.8 μL Cell-Tak, 5.9 μL 1 M NaOH and 336.3 μL 0.1 M $NaHCO_3$) to attach the cells. Subsequently, $1x10^6$ cells were transplanted to the FluoroDish (World Precision Instruments Inc. China) and stood for 2 min so that the cells could sufficiently stick to the bottom of the petri dish. Finally, the moderate culture medium (RPMI) and microbead diluent were added to the petri dish.

Before the indentation measurement, the relationship between the applied

laser power, the trap stiffness and sensitivity were calibrated followed by the standard calibration procedure as suggested in the equipment manual. The constants, including the trap stiffness k and sensitivity S, was fitted and calculated by the control program of the optical tweezers based on the recorded thermal motion of the trapped microbead.

The typical indentation measurement was carried out as follows: first, the microscope's focal plane was adjusted to observe the most explicit cell edge. Then, the laser focus was carefully adjusted to ensure that the laser trap and the microbead are in the same focal plane. By moving the sample stage, the cell to be indented was moved towards the trapped bead until it reached the contact. The purpose of moving the stage instead of the bead is to minimize measurement errors since it is rather difficult to accurately determine the position of bead while it is being moved at high speed; moreover, the viscous drag force applied on the microbeads during the moving might also influence measurement. The initial contact between the bead and the cell is identified by the sudden change of laser signal D recorded. After solid contact is reached, the movement of stage Z and its corresponding laser signal change ΔD is continuously recorded. Here, the force applied between the bead and the cell is equal to the laser trapped force applied on the bead, which is given by:

$$P = \Delta D \cdot S \cdot k \tag{1}$$

and the actual indentation displacement of the bead into the cells h is

$$h = Z - \Delta D \cdot S \quad (2)$$

The recorded Z and D will be transferred to force and depth data the same as those in traditional indentation test according to Eq. (1) and (2).

All the optical tweezers indentation test following identical protocol, i.e., indent into the cell surface at constant load rate 1 μm/s until the Z value reaches 1 μm, hold at peak load for 10s and then unload at 1 μm/s for 10s to ensure sufficient data points be collected for further analysis.

Calculation of Young's modulus of leukemia cells

The cells are highly viscoelastic. To accurately determine the elastic modulus of cells, rate-jump method that can eliminate the viscoelastic effects during the analysis was adopted for the elastic modulus measurement. According to the rate-jump method, the elastic contact stiffness S_e for an indentation test is

$$S_e = 2aE_r = \frac{\Delta \dot{P}}{\Delta \dot{h}} \quad (3)$$

Here, $\Delta\dot{P}$ and $\Delta\dot{h}$ are the nets of loading rate and indentation displacement rate just before and after the unloading point, respectively. The a is the contact radius of the bead-cell contact. In this particular case, in which the spherical bead is used, $\alpha = \sqrt{Rh_u}$, and Eq. (3) can be converted to

$$E_r = \frac{\dot{P_u} - \dot{P_h}}{2(\dot{h_u} - \dot{h_h})\sqrt{Rh_u}} \quad (4).$$

The elastic modulus of cells can be calculated from the following equation after the reduced modulus E_r is obtained:

$$\frac{1}{E_r} = (\frac{1-\nu^2}{E})_{sample} + (\frac{1-\nu^2}{E})_{indenter} \quad (5)$$

where the Poisson ratio ν for the cell in this work is chosen to be 0.5. Moreover, the indenter (microbead) is made of polystyrene, and its elastic modulus is 3-3.6 GPa, which is much larger than that of the cells. $(1-\nu^2)/E$ for the indenter is so small that it can be reasonably neglected.

Cell structure observation

To observe the cytoskeleton of leukemia cells after drug treatment, laser scanning confocal microscope (LSCM, Leica, German) was applied to visualize the cytoskeleton protein and nucleus. After 24h drugs treatment, the leukemia cells adhered to a creep plate by Cell-Tak and fixed with 4% formaldehyde (Beyitime, China) for 30 min. After rinsing twice with PBS, the cells were permeabilized with 0.5% Triton X-100 in PBS for 10 min, then stained with FITC-conjugated phalloidin (1:200) (Beyitime, China) for 20 min to visualize filaments of β-actin. Cell nuclei were stained by incubating the samples with 1 μg/ml 40, 60-diamidino-2-phenylindole (DAPI, Beyitime, China) in PBS for the 30s, then washed three times with PBS to remove the residual dye. The images were acquired using an LSCM

and processed by Image J.

Real-Time PCR analysis

Total RNA was isolated from four drug treatment groups: 0.1 μM CTX, 1 μM DEX, 10 μg/L PMA, and 1 μM ATRA and one untreated control group, by using RNAiso Plus (TaKaRa). Then the total RNA was used to synthesize cDNA by using the cDNA Synthesis Kit (Beyotime, China). Real-Time PCR was performed with an SYBR Green Real-time PCR Master Mix kit (TaKaRa, Japan). The reaction volume of the qRT-PCR reactions was 20 μL, containing forward and reverse primers (0.4 μM), 2 μL template DNA, 10 μL SYBR® Green Real-time PCR Master Mix and 6.4 μL ddH_2O. Real-Time PCR was performed on an Applied Biosystems, StepOnePlus Instrument (U. S. A.), and the cycling programs were as follows: 95°C for 5 min pre-degeneration, followed by 40 cycles of amplification at 95°C for 15 min and 60°C for 60 sec, then 95°C for 15 sec. The gene expression level was normalized by β-actin, and ΔΔCT was calculated by referring to the control group. All the primers were designed online by PrimerBank (https://pga.mgh.harvard.edu/primerbank/). α-tubulin forward primer sequence: TCGATATTGAGCGTCCAACCT; reverse primer sequence: CAAAGGCACGTTTGGCATACA. Vimentin forward primer sequence: TGCCGTTGAAGCTGCTAACTA; reverse primer sequence: CCAGAGGGAGTGAATCCAGATTA. Lamin A/C forward primer sequence: AATGATCGCTTGGCGGTCTAC; reverse primer

sequence: CACCTCTTCAGACTCGGTGAT. β-actin forward primer sequence: TGACGTGGACATCCGCAAAG; reverse primer sequence: CTGGAAGGTGGACAGCGAGG.

Transwell migration assay

Cell migration ability was measured using a transwell chamber (8 μm pore size, Corning, U. S. A.) with Matrigel (Corning, U. S. A.). Transwell chambers were placed into 24-well plates and coated with 30 μL Matrigel, then incubated at 37°C for 3h. The drug treatment groups and the control group were synchronized for 3h aimed to sensitive to serum. The cells were seeded at a density of $1x10^5$ cells/well in the 200 μL serum-free RPMI and 0.1% BSA for equilibrium osmotic pressure in the upper inserted chambers. Meanwhile, 600 μL of 10% FBS-RPMI was added to the lower chambers. After 24h, cells that migrated to the lower compartments of the Boyden chamber were counted under a light microscope with a blood counting chamber.

Statistical analysis

All data were analyzed by the Standard t-test and were expressed as the mean ± standard error of the mean. Data were analyzed using GraphPad Prism 5 software for Windows and differences were considered statistically significant when p-value less than 0.05.

RESULTS

Young's modulus of K562 is increased three-fold after PMA treatment

The cytoskeleton protein, e.g., F-actin and microtubules, which has a significant influence on the mechanical properties of cells, had a different expression and contribution on the mechanical properties in the different cell cycle[22]. With the purpose to identify the possible influence of phase difference on the cell mechanical properties, the cells were synchronized to the G0 phase. The optical tweezers indented randomly on selected K562 cells. From Figure 1.a, we can observe that the phase-controlled (30.47 ± 6.61 Pa) had a lower and more stable Young's modulus than the phase-mixed (35.60 ± 17.45 Pa). Since the results of the control experiment suggested that the phase-controlled cells should have more consistent mechanical properties, in the following tests, all the drug treatment proceeded by phase control principle. The Young's modulus of K562 treated with different drugs is shown in Fig. 1.b and Table 1. The results indicate that Young's modulus of the cells treated with PMA (99.95 Pa) is a nearly three-fold increased compared to the control (30.47 Pa). As for the other three treatments (DEX, ATRA, and CTX), Young's modulus is almost the same as the control (Fig. 1.b, Table 1)

Vimentin is overexpressed in K562 after PMA treatment

The cell cytoskeleton and nucleus skeleton are the most critical components which provide the mechanical properties for cells. To explore the reason of the elastic modulus's variation for leukemia cells, the

structure of the membrane and nucleus were investigated by LSCM (Figure 2). It was found that the fluorescence intensity of the cytoskeleton has an increase for PMA and ATRA treatment and a small decrease for CTX and DEX treatment (Figure 2.f). However, the nucleus-cytoplasmic ratio has a small increase for all of the drugs treatment (Figure 2.g).

To further illuminate the reason why the elastic modulus of leukemia cell K562 increased after PMA treatment, we analyzed the mRNA levels of cell cytoskeleton protein vimentin and α-tubulin and cell nucleus membrane protein lamin A/C after drug treatments (Fig. 3). The expressions of cytoskeleton protein vimentin and α-tubulin were the highest for PMA treatment among all the drugs treatments and control sample (Fig. 3.a and b). The other drugs treatments also had a different influence on the expression of vimentin and α-tubulin with no significance different, except α-tubulin 0.5-fold decrease after DEX treatment (Fig. 3.a and b). Compared with the control group, all the four drugs treatments have a slight increase in the expression of nucleus membrane protein lamin A/C (Fig. 3.c).

Migration ability of leukemia cells k562 is decreased after PMA treatment

It was known that the deformability of leukemia cells was the reflex of their elastic modulus, and related to their metastasis or leukostasis. In order to validate the significance of elastic modulus on metastasis or leukostasis,

the migration ability of K562 with PAM treated was characterized by a transwell assay. Results are presented in Fig. 4. It was shown that there was a reduction of migration ability of K562 in the transwell assay after 24h treatment of PMA. It was suggested that PMA treatment might decrease the leukemia cells migration, and even lead to leukostasis in some capillary vessels through the increase of the elastic modulus of cells (Fig. 1.b).

DISCUSSION

The biomechanical properties of cells were tightly related to their physiological/pathophysiological variation and metabolic states, especially in some pathological states, e.g., cancer initiation or metastasis[23,24]. Some studies had shown that leukemia cells were stiffer than normal leukocyte[12]. When leukemia cells proliferated in the blast or treated by drugs, e.g., PMA would lead to a severe symptom leukostasis[25]. Pinkhas et al. found that intravenous infusion of PMA triggered a severe degree of pulmonary leukostasis in rabbits *in vivo*[26]. In our study, the stiffness of k562 cells after PMA treatment was almost threefold higher than that of the control. Some researchers had found that the stiffer the leukemia cells, the higher the risk of leukostasis was[2]. In this work, the migration ability of k562 cells also decreased for PMA treatment compared to the control. It was found that stiffer the cells are, the lower the deformability, and the slower the migration was. This agreed with another hypothesis that the migration of

leukemia cells were tightly linked with symptom leukostasis[27].

Fletcher et al. had explored AFM to measure the deformability of K562 cell through placing cells in micro-fabricated wells so that the cells could be fixed to conduct indentation[12]. Sulchek et al. also employed the AFM to measure Young's modulus of leukemia cell K562 and used the Hertzian model to calculate out the average modulus of K562 cells were 420 ± 380 Pa[17]. However, the stiffness obtained by them showed a large scattering range, and the value was much larger than the result obtained in our study. The reason was that the AFM has a nanoscale cantilever tip (about 10 nm), which is comparable to the diameter of a single actin microfilament (6-8 nm)[28]. The AFM tip might indent individual microfilament or nano-scaled holes surrounded by microfilament. As a result, the scattering range was extensive, which was comparable with the average value. However, the microbeads used in OT had a diameter (3 μm), which is in the same magnitude of the size of the cells (from 8-20 μm), so the elastic modulus obtained by OT could represent the whole cytoskeletal mechanical deformability rather than the local microfilament or hole. From Fig. 1 and table 1, the scattering range of elastic modulus by OT (30.47 ± 6.61 Pa)was much smaller than the data obtained by AFM (420 ± 380 Pa), and the value was also smaller than the other measurements[18,29,30].

It is well known that living cells are viscoelastic. Therefore, the overall force-displacement response obtained in the measurement represented the

viscoelastic properties of cells, no matter whether the experimental platform is an indentation, suction or traction[31]. A viscoelastic material governed by a constitutive law in which linear elastic springs were connected to (in general) non-linear viscous dashpots were forming any network arrangement, the response during a sudden jump in the loading or strain rate is governed only by that of the elastic springs, while the dashpots behave completely rigidly[20,21,32]. Based on this theory, we only analyzed the force-displacement response around the step unloading time as a jump, then the modulus measured this way would be specific to the moment at which the rate jump was imposed but would be independent of magnitude of the rate jump at that time point, i.e., it would be an intrinsic material property[33]. The rate-jump model could eliminate the viscoelastic effect of cells and precisely calculate the elastic modulus.

The Young's modulus of K562 had almost a three-fold increase treated by PMA compared with the untreated one, the other drugs DEX, ATRA, and CTX had no significant influence on Young's modulus of cells. PMA was able to make myeloid leukemia cells, such as K562, and HL60, to differentiate into megakaryocytic or even induce apoptosis, which would both modify the cytoskeleton to alter the deformability of the cells[34]. PMA would rearrange the cytoskeleton to increase Young's modulus of the K562 cells. ATRA could arrest the cell cycle in C0/G1 phase and induce the cell to differentiate into a granulocytic lineage[35,36]. The effects of differentiation

into the granulocytic lineage, which was suspension phase as the K562, was different from differentiation into the megakaryocytic lineage that belongs to the adhesion phase. Therefore, K562 cells treated with ATRA should not alter the cytoskeleton and also the deformability of the cells. DEX was an anti-inflammatory drug widely used in acute lymphoblastic leukemia to reduce the pathogenesis of leukostasis[37]. DEX also could be used as a chemosensitizer in combination with intensive chemotherapy to treat the myeloid leukemia cells and reduce the risk of leukostasis[38]. In our study, we found that the DEX did not change the cytoskeleton and Young's modulus of the K562 cells. DEX might change the adhesion of cell-cell or cell-substrate to achieve the reduce the risk of leukostasis. CTX often combined with other drugs to treat leukemia cells through inhibiting proliferation[39]. Here, we found that Young's modulus of K562 cells treated with CTX was not changed compared with the untreated ones. The CTX would not change the cytoskeleton of the K562 cells in the dose of our research.

Vimentin was a cytoskeleton protein and had been reported to be involved in the migration of monocytes across the endothelium walls and was associated with cell adhesion by regulating the expression and the distribution of adhesion molecules[40-42]. Some researchers had found that the leukemia cells show an increase in the adhesion ability and a decrease in the migration ability through high expression vimentin after PMA

treatment[43]. Here, we found that vimentin was not only associated with cell adhesion but also tightly in related to cell deformability through the PMA treatment.

The migration ability of the leukemia cells was an essential factor for the organ infiltration, relapse, and leukostasis, which still correlated with poor prognosis[44]. Migration was in accordance with the deformability and adhesion ability of cells. Zhou et al. had found that the leukemia cells showed a strong adhesion to the substrate and a weak migration which led to the cells be stuck to the substrate with PMA treatment[43]. Andrew et al. also found that chemotherapy-induced stiffening in leukemia cell leading to an increase in transit times through *in vitro* microcirculation[45]. The increase of leukostasis risk was due to the transit time increased in the capillary vessel. In this work, the migration ability showed a significant decrease under PMA treatment which led to a high risk of leukostasis.

CONCLUSION

In this work, the elastic modulus of leukemia cells for different drug treatments was precisely measured through optical tweezers and calculated by the rate-jump model. The elastic modulus of leukemia cells k562 was threefold increased with PMA treatment. Also, the migration of leukemia cells K562 was vigorously decreased under PMA treatment. From the results of qPCR, the cytoskeleton vimentin protein was up-regulated

expressed which tightly associated with the elastic modulus increase. From this work, we can learn that the PMA would induce leukemia cells K562 to become stiffer and experience weaker migration through changing the expression of the cytoskeleton protein vimentin, and maybe lead to a severe side effect leukostasis in clinical.

ACKNOWLEDGEMENT

This study is financially supported by National Foundation of Science and Technology (Project No. 11872200), Guangdong Foundation of Science and Technology (Project No. 2017B030301018), Shenzhen Science and Technology Innovation Committee (Project No. JCYJ20160517160827379, JCYJ20170817111312887 and ZDSYS20140509142721429).

Author Contributions

B. Tang designed the study; K. Wang and Y. Xues performed and interpreted indentation measurement and confocal analysis; K. Wang and Y. Peng performed and interpreted RT-PCR analysis; K. Wang and Y. Zhang performed and interpreted transwell analysis; K. Wang wrote the manuscript; X. Pang and L. Ruiz-Ortega revised the manuscript; A.H.W. Ngan and B. Tang directed and supervised the research. All authors approved the final manuscript.

Conflict of interest statement

The authors declare no competing financial interest.

REFERENCES

1. Röllig C, Ehninger G. How I treat hyperleukocytosis in acute myeloid leukemia. *Blood*. 2015;125(21):3246-3252.
2. Lam WA, Rosenbluth MJ, Fletcher DA. Increased leukaemia cell stiffness is associated with symptoms of leucostasis in paediatric acute lymphoblastic leukaemia. *Br J Haematol*. 2008;142(3):497-501.
3. Swaminathan V, Mythreye K, O'Brien ET, Berchuck A, Blobe GC, Superfine R. Mechanical stiffness grades metastatic potential in patient tumor cells and in cancer cell lines. *Cancer Res*. 2011;71(15):5075-5080.
4. Smolyakov G, Thiebot B, Campillo C, et al. Elasticity, Adhesion, and Tether Extrusion on Breast Cancer Cells Provide a Signature of Their Invasive Potential. *ACS Appl Mater Inter*. 2016;8(41):27426-27431.
5. Xu W, Mezencev R, Kim B, Wang L, McDonald J, Sulchek T. Cell stiffness is a biomarker of the metastatic potential of ovarian cancer cells. *PLoS One*. 2012;7(10):e46609.
6. Sant GR, Knopf KB, Albala DM. Live-single-cell phenotypic cancer biomarkers-future role in precision oncology? *NPJ Precis Oncol*.

2017;1(1):21.

7. Zhou ZL, Sun XX, Ma J, et al. Actin cytoskeleton stiffness grades metastatic potential of ovarian carcinoma Hey A8 cells via nanoindentation mapping. *J Biomech*. 2017;60:219-226.
8. Matulic M, Skelin J, Radic-Kristo D, Kardum-Skelin I, Grcevic D, Antica M. Notch affects the prodifferentiating effect of retinoic acid and PMA on leukemic cells. *Cytom Part A*. 2015;87(2):129-136.
9. Lopes EC, Garcia MG, Vellon L, Alvarez E, Hajos SE. Correlation between decreased apoptosis and multidrug resistance (MDR) in murine leukemic T cell lines. *Leuk Lymphoma*. 2001;42(4):775-787.
10. Ojima Y, Duncan MT, Nurhayati RW, Taya M, Miller WM. Synergistic effect of hydrogen peroxide on polyploidization during the megakaryocytic differentiation of K562 leukemia cells by PMA. *Exp Cell Res*. 2013;319(14):2205-2215.
11. Kumar S, Weaver VM. Mechanics, malignancy, and metastasis: the force journey of a tumor cell. *Cancer Metas Rev*. 2009;28(1-2):113-127.
12. Rosenbluth MJ, Lam WA, Fletcher DA. Force Microscopy of Nonadherent Cells: A Comparison of Leukemia Cell Deformability. *Biophys J*. 2006;90(8):2994-3003.
13. Esteban-Manzanares G, Gonzalez-Bermudez B, Cruces J, et al. Improved Measurement of Elastic Properties of Cells by Micropipette

Aspiration and Its Application to Lymphocytes. *Ann Biomed Eng*. 2017;45(5):1375-1385.

14. Féréol S, Fodil R, Labat B, et al. Sensitivity of alveolar macrophages to substrate mechanical and adhesive properties. *Cell Motil*. 2006;63(6):321-340.
15. Wirtz D. Particle-Tracking Microrheology of Living Cells: Principles and Applications. *Annu Rev Biophys*. 2009;38(1):301-326.
16. Hou J, Luo T, Ng KL, Leung AY, Liang R, Sun D. Characterization of Drug Effect on Leukemia Cells Through Single Cell Assay With Optical Tweezers and Dielectrophoresis. *IEEE Trans Nanobiosci*. 2016;15(8):820-827.
17. Islam M, Mezencev R, McFarland B, et al. Microfluidic cell sorting by stiffness to examine heterogenic responses of cancer cells to chemotherapy. *Cell Death Dis*. 2018;9(2):239-251.
18. Lam WA, Rosenbluth MJ, Fletcher DA. Chemotherapy exposure increases leukemia cell stiffness. *Blood*. 2007;109(8):3505-3508.
19. Zheng Y, Wen J, Nguyen J, Cachia MA, Wang C, Sun Y. Decreased deformability of lymphocytes in chronic lymphocytic leukemia. *Sci Rep*. 2015;5:7613-7618.
20. Zhou ZL, Hui TH, Tang B, Ngan AHW. Accurate measurement of stiffness of leukemia cells and leukocytes using an optical trap by a rate-jump method. *Rsc Advances*. 2014;4(17):8453-8460.

21. Ngan AHW, Tang B. Response of power-law-viscoelastic and time-dependent materials to rate jumps. *J Mater Res*. 2011;24(3):853-862.
22. Tsai MA, Waugh RE, Keng PC. Cell cycle-dependence of HL-60 cell deformability. *Biophys J*. 1996;70(4):2023-2029.
23. Yu H, Mouw JK, Weaver VM. Forcing form and function: biomechanical regulation of tumor evolution. *Trends Cell Biol*. 2011;21(1):47-56.
24. Coughlin MF, Bielenberg DR, Lenormand G, et al. Cytoskeletal stiffness, friction, and fluidity of cancer cell lines with different metastatic potential. *Clin Exp Metast*. 2013;30(3):237-250.
25. Hirata F, Yoshida M, Ogura Y. High glucose exacerbates neutrophil adhesion to human retinal endothelial cells. *Exp Eye Res*. 2006;82(1):179-182.
26. Berliner S, Weinberger M, Ben-Bassat M, et al. Amphotericin B causes aggregation of neutrophils and enhances pulmonary leukostasis. *Am Rev Respir Dis*. 1985;132(3):602-605.
27. Stucki A, Rivier AS, Gikic M, Monai N, Schapira M, Spertini O. Endothelial cell activation by myeloblasts: molecular mechanisms of leukostasis and leukemic cell dissemination. *Blood*. 2001;97(7):2121-2129.
28. Winkelman JD, Suarez C, Hocky GM, et al. Fascin- and α-Actinin-Bundled Networks Contain Intrinsic Structural Features that Drive

Protein Sorting. *Curr Biol*. 2016;26(20):2697-2706.

29. Lange JR, Goldmann WH, Alonso JL. Influence of alphavbeta3 integrin on the mechanical properties and the morphology of M21 and K562 cells. *Biochem Biophys Res Commun*. 2016;478(3):1280-1285.
30. Wang G, Crawford K, Turbyfield C, Lam W, Alexeev A, Sulchek T. Microfluidic cellular enrichment and separation through differences in viscoelastic deformation. *Lab Chip*. 2015;15(2):532-540.
31. Li QS, Lee GY, Ong CN, Lim CT. AFM indentation study of breast cancer cells. *Biochem Biophys Res Commun*. 2008;374(4):609-613.
32. Tang B, Ngan AHW. A rate-jump method for characterization of soft tissues using nanoindentation techniques. *Soft Matter*. 2012;8(22):5974-5979.
33. Zhou ZL, Tang B, Ngan AHW. The Biomachanics of Drug-Treated Leukemia Cells investigated Using Optical Tweezers. *Nano LIFE*. 2012;02(01):125-131.
34. Tringali C, Lupo B, Cirillo F, et al. Silencing of membrane-associated sialidase Neu3 diminishes apoptosis resistance and triggers megakaryocytic differentiation of chronic myeloid leukemic cells K562 through the increase of ganglioside GM3. *Cell Death Differ*. 2009;16(1):164-174.
35. Liu WJ, Zhang T, Guo QL, Liu CY, Bai YQ. Effect of ATRA on the expression of HOXA5 gene in K562 cells and its relationship with cell

cycle and apoptosis. *Mol Med Report*. 2016;13(5):4221-4228.

36. Kohroki J, Fujita S, Itoh N, et al. ATRA-regulated Asb-2 gene induced in differentiation of HL-60 leukemia cells. *FEBS Lett*. 2001;505(2):223-228.
37. Inaba H, Pui CH. Glucocorticoid use in acute lymphoblastic leukaemia. *Lancet Oncol*. 2010;11(11):1096-1106.
38. Bertoli S, Picard M, Berard E, et al. Dexamethasone in hyperleukocytic acute myeloid leukemia. *Haematologica*. 2018;103(6):988-998.
39. Byrd JC, Kipps TJ, Flinn IW, et al. Phase 1/2 study of lumiliximab combined with fludarabine, cyclophosphamide, and rituximab in patients with relapsed or refractory chronic lymphocytic leukemia. *Blood*. 2010;115(3):489-495.
40. Nieminen M, Henttinen T, Merinen M, Marttila–Ichihara F, Eriksson JE, Jalkanen S. Vimentin function in lymphocyte adhesion and transcellular migration. *Nat Cell Biol*. 2006;8:156-162.
41. Carman CV, Springer TA. A transmigratory cup in leukocyte diapedesis both through individual vascular endothelial cells and between them. *J Cell Bio*. 2004;167(2):377-388.
42. Yao W, Huang L, Sun Q, et al. The inhibition of macrophage foam cell formation by tetrahydroxystilbene glucoside is driven by suppressing vimentin cytoskeleton. *Biomed Pharmacother*. 2016;83:1132-1140.
43. Zhou ZL, Ma J, Tong MH, Chan BP, Wong AS, Ngan AH.

Nanomechanical measurement of adhesion and migration of leukemia cells with phorbol 12-myristate 13-acetate treatment. *Int J Nanomedicine*. 2016;11:6533-6545.

44. Velazquez-Avila M, Balandran JC, Ramirez-Ramirez D, et al. High cortactin expression in B-cell acute lymphoblastic leukemia is associated with increased transendothelial migration and bone marrow relapse. *Leukemia*. 2018.
45. Prathivadhi-Bhayankaram SV, Ning J, Mimlitz M, et al. Chemotherapy impedes in vitro microcirculation and promotes migration of leukemic cells with impact on metastasis. *Biochem Biophys Res Commun*. 2016;479(4):841-846.

Figure 1. The Young's modulus of k562 cells. (a) The Young's modulus of k562 cells in G0 phase or randomly. Control: synchronized to the G0 phase of the k562 cells; Mix: phase randomly of the k562 cells. N ≥ 20. (b) The Young's modulus of k562 cells after different drugs treatment. PMA: phorbol 12-myristate 13-acetate, ATRA: all-trans retinoic acid, CTX: Cytoxan, and DEX: Dexamethasone. N ≥ 20.

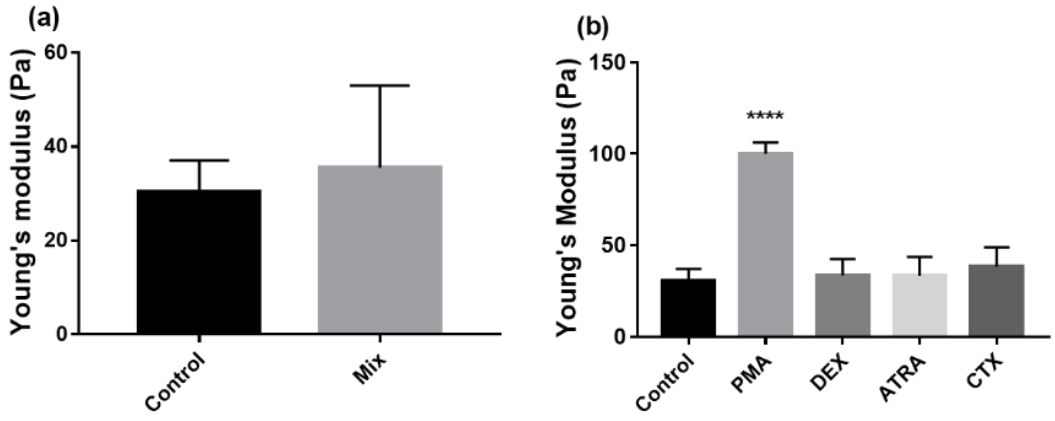

Figure 2 The fluorescence images of leukemia cell k562 under different treatment and the data analysis.(a): Control; (b): ATRA; (c): CTX; (d): DEX; (e): PMA; (f): the fluorescence intensity mean value of phalloidine; (g): the nucleo-cytoplasmic ratio. *p<0.05.

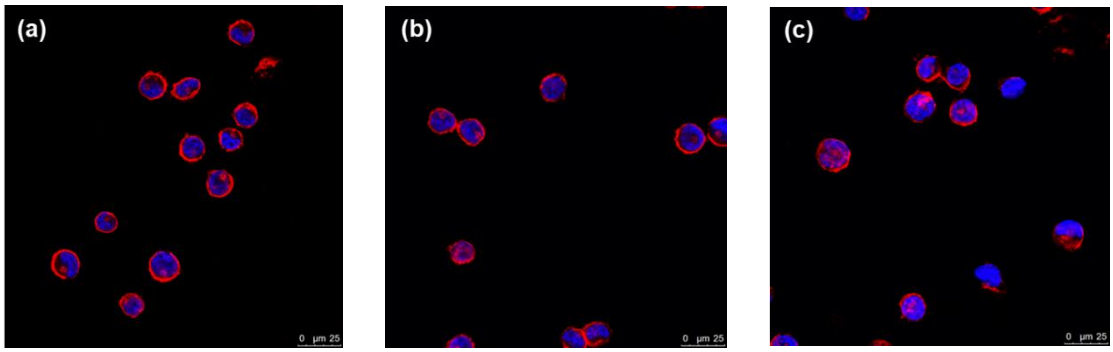

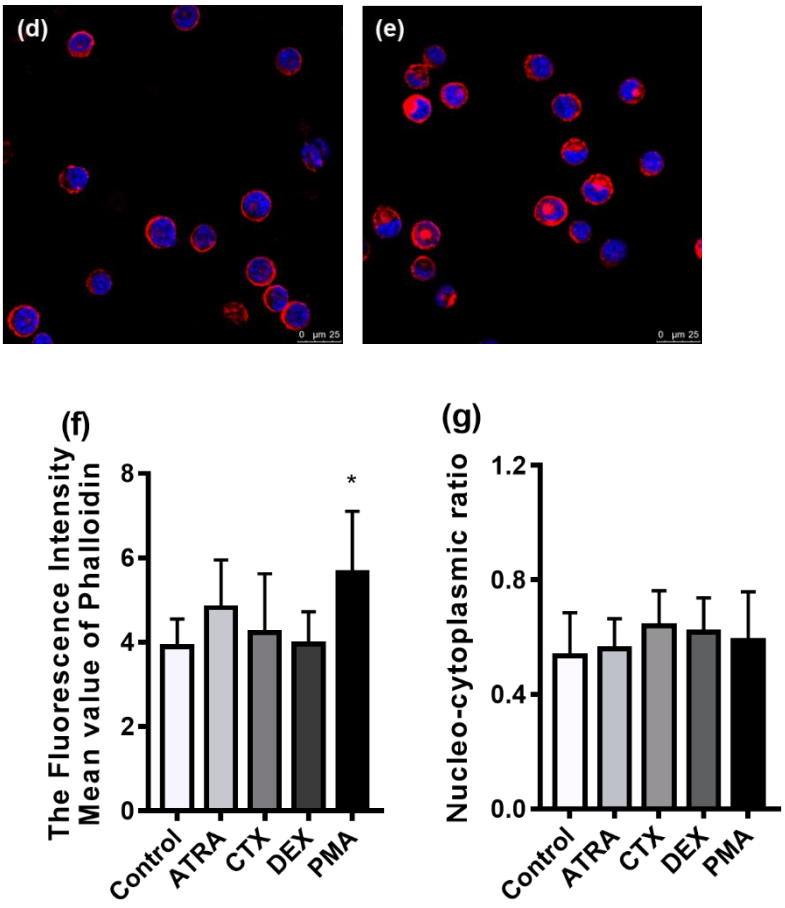

Figure 3 The gene expression of leukemia cell k562 under different drugs treatments. (a) The gene expression of α-tubulin after PMA, ATRA, CTX and PMA treatment and control. (b) The gene expression of vimentin after PMA, ATRA, CTX and PMA treatment and control. (c) The gene expression of lamin A/C after PMA, ATRA, CTX and PMA treatment and control. ****p<0.0001.

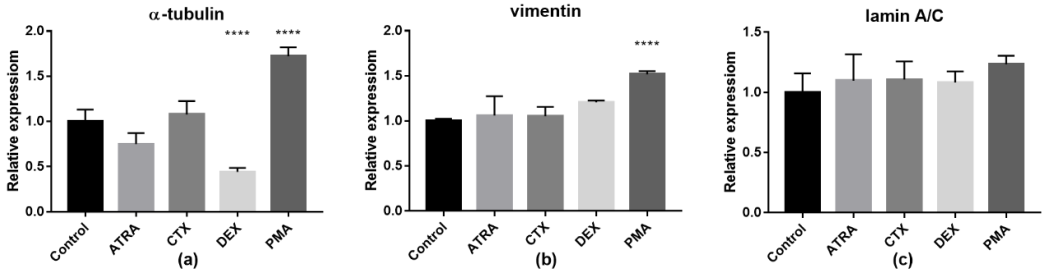

Figure 4. Relative migration ability of k562 cells after drugs treatment.

**p<0.01, ****p<0.0001.

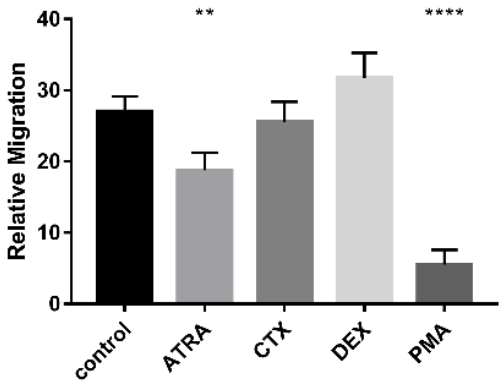

Table 1 Average and standard deviation value of the elastic modulus of k562 cells (*n≥20)

	$E_{average}$ (Pa)	STD (Pa)
Control	30.47	6.61
PMA	99.95	6.27
DEX	33.42	8.97
ATRA	33.22	10.33
CTX	38.31	10.45